JOUL, Volume *4*

Supplemental Information

Solid Acid Electrochemical Cell

for the Production of Hydrogen from Ammonia

Dae-Kwang Lim, Austin B. Plymill, Haemin Paik, Xin Qian, Strahinja Zecevic, Calum R.I. Chisholm, and Sossina M. Haile

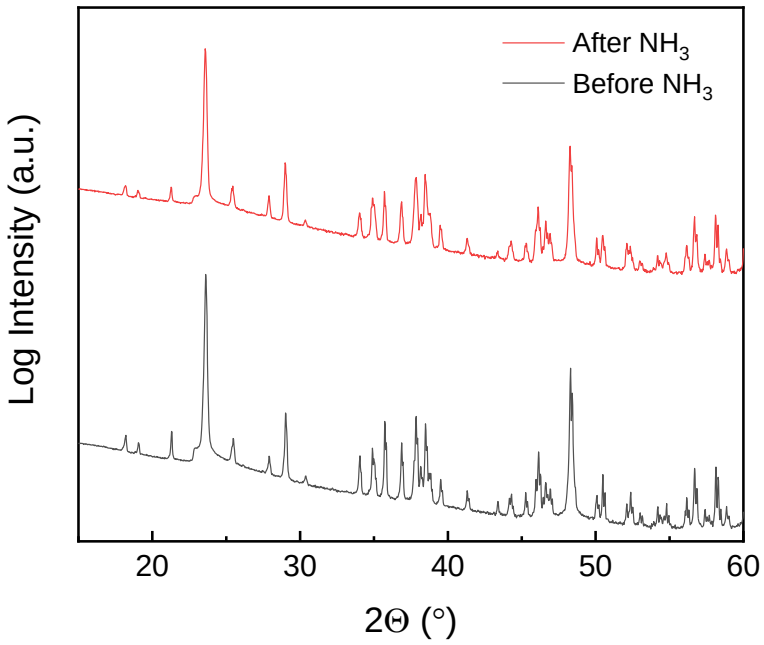

Figure S1. X-ray powder diffraction patterns (Rigaku SmartLab) of CsH_2PO_4: before (as-received) and after exposure to flowing humidified NH_3 for 24 h at 250 °C (pNH_3 = 0.4 atm, pH_2O = 0.38 atm, balance N_2; total gas flow rate = 50 sscm). The electrolyte is stable against reaction with ammonia at the cell operating conditions.

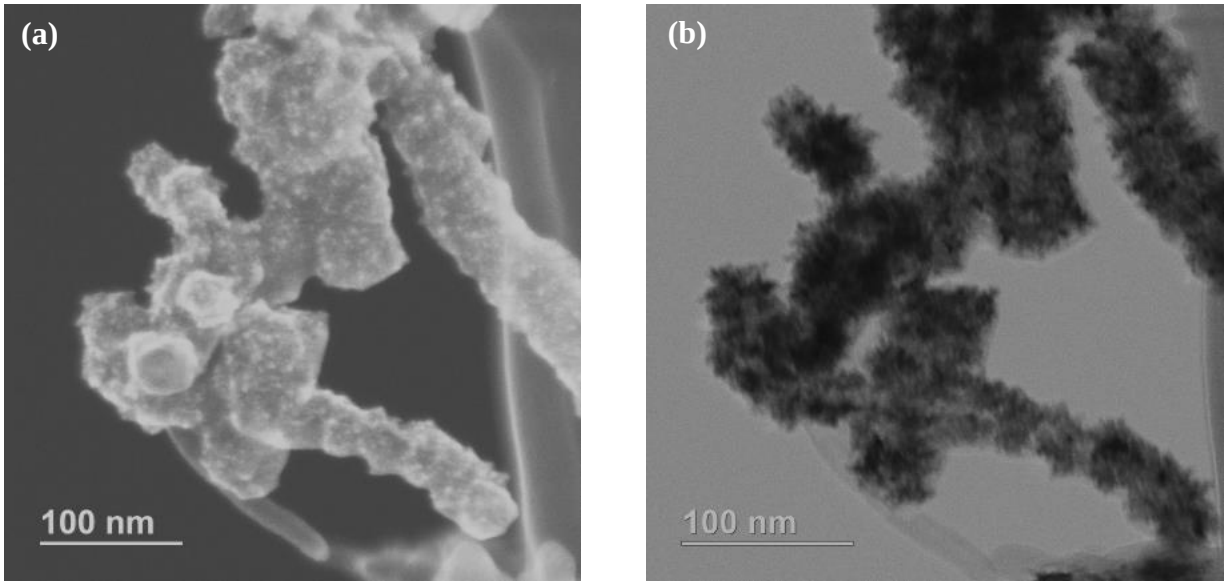

Figure S2. Scanning Transmission Electron Microscopy (STEM) images of 60wt% Ru/CNT: (a) secondary electron (SE) image, and (b) phase contrast (TE) image (Hitachi HD2300). The Ru (deposited onto the multiwall carbon nanotubes by the procedures outlined in the main text) has an average particle size of less than 10 nm and fully coats the multiwalled CNTs.

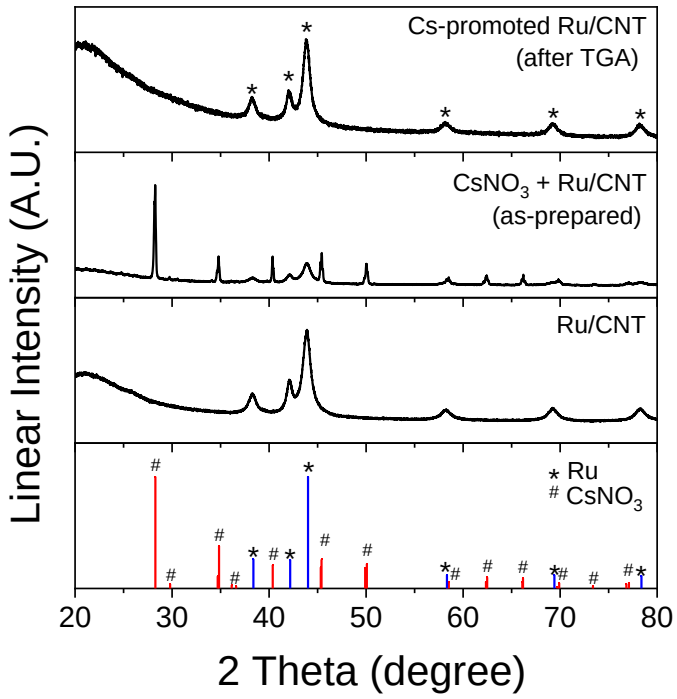

Figure S3. X-ray diffraction patterns (Rigaku Ultima IV) collected from catalyst materials: (bottom) 60wt% Ru/CNT as prepared; (middle) 60wt% Ru/CNT with $CsNO_3$ promotor, as prepared; and (top) Cs-promoted 60wt% Ru/CNT after thermogravimetric analysis (Figure S4). The breadth of the peaks in the Ru/CNT material indicates a crystallite size of ~ 7 nm. Crystalline $CsNO_3$ results from the initial deposition of the promotor (middle). After thermal analysis (which includes heat treatment at 250 °C under H_2), the Cs bearing phase is amorphous (top).

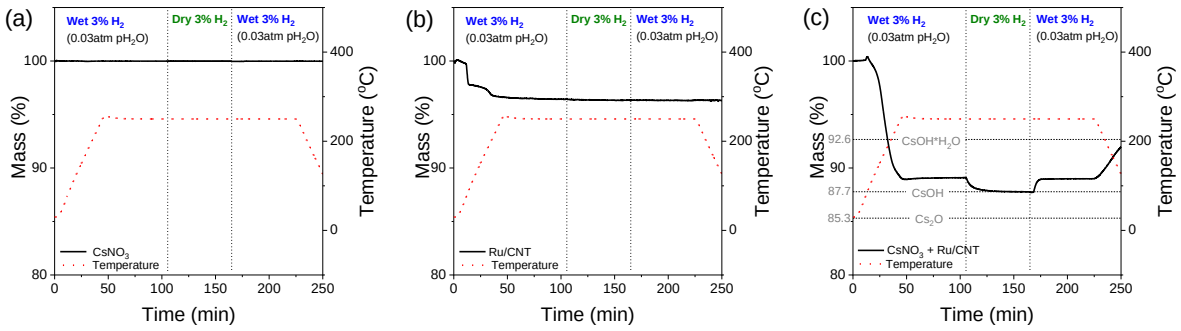

Figure S4. Thermogravimetric analysis (Netzsch STA 443) of catalyst materials: (a) as-received commercial $CsNO_3$; (b) in-house prepared 60 wt% Ru/CNT; and (c) 60 wt% Ru/CNT treated with $CsNO_3$. Gas atmosphere of measurements as indicated. In (a) examined alone, $CsNO_3$ shows no weight loss under hydrogen up to 250 °C. Mass loss from Ru/CNT in (b) is due to reduction of ruthenium and removal of surface sorbed species. Mass loss from Ru/CNT treated with $CsNO_3$ in (c) is consistent with the transformation of $CsNO_3$ to CsOH, revealing that in the presence of Ru, $CsNO_3$ decomposes.

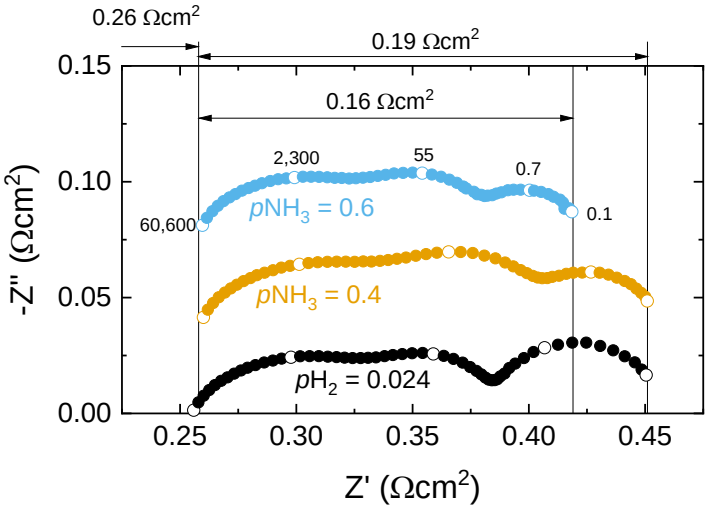

Figure S5. Electrochemical impedance spectra. Data at open circuit conditions for a representative electrochemical cell (Cell 1) measured at 250 °C with humidified hydrogen supplied to the counter electrode (pH_2O = 0.38 atm) and the indicated gas (humidified) supplied to the working electrode, with pH_2O = 0.38 atm and balance Ar and N_2 (Biologic SP-300, voltage amplitude of 20 mV). Spectra are offset along the imaginary axis for clarity. Frequency values (Hz) indicated for selected data. The ohmic resistance is 0.26 Ωcm^2 under all three conditions. The electrochemical reaction resistances under dilute hydrogen and under pNH_3 = 0.4 atm are similar, and are in turn, slightly larger than under pNH_3 = 0.6 atm.

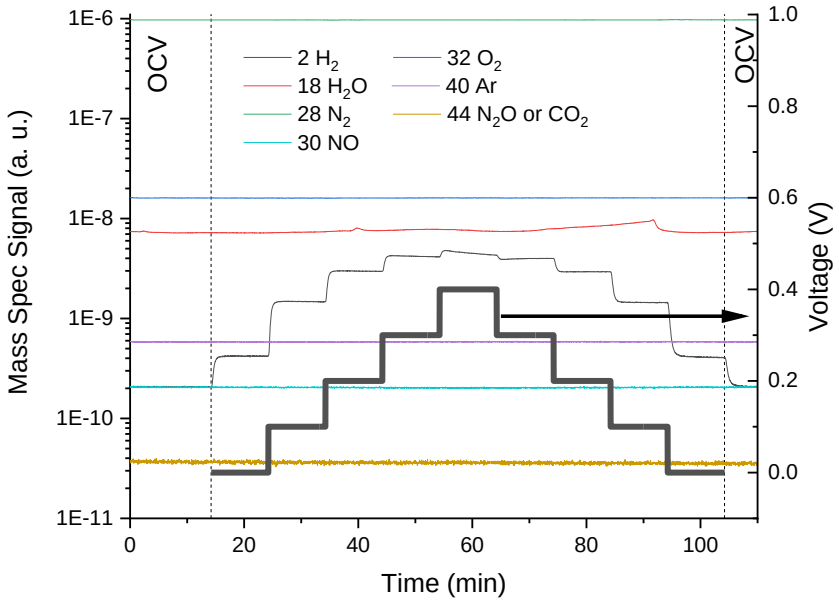

Figure S6. **Purity of the H_2 stream**. Shown is thetime evolution of mass spectrometry signals of relevant species in the gas evolved from the cathode as part of the Faradaic efficiency measurement reported in Figure 2(b) of the main text. Measurement was performed with humidified ammonia, pNH_3 = 0.4, pH_2O = 0.38, balance N_2, supplied to the working electrode. In contrast to cell performance studies, humidified N_2 (pH_2O = 0.38 atm) was supplied to the counter electrode, rather than H_2, so as to ensure detection of only electrochemically evolved hydrogen and avoid drift of a high H_2 baseline in the mass spectrometer (Thermostar Pfeiffer GSD 301 T2). These conditions generate an open circuit voltage < 0 and H_2 production at V = 0. Removal of H_2O from the cathode exhaust was achieving by passing it through a condenser, which would have also removed any ammonia. Absence of ammonia in the generated H_2 was established by measuring the pH of the H_2O trapped in the condenser, which was found to be 7.

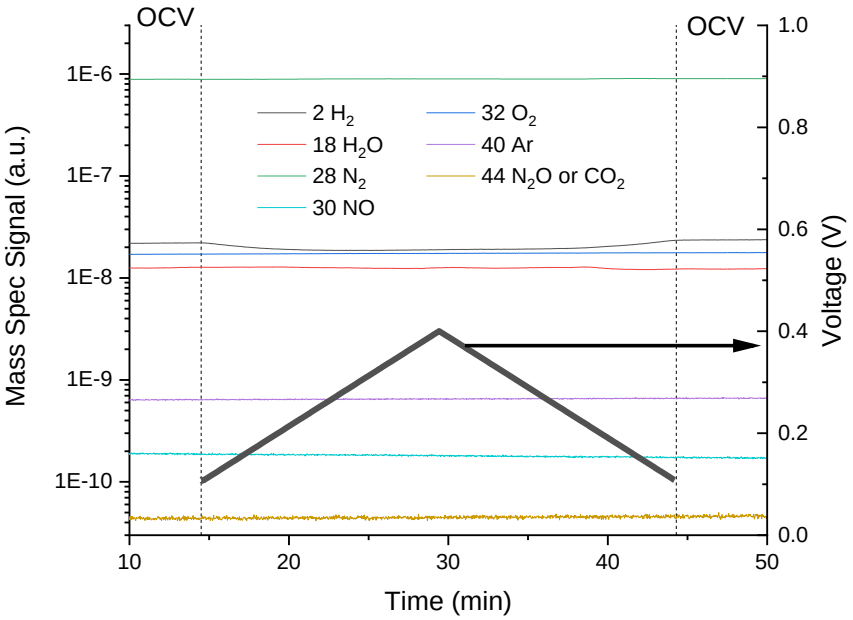

Figure S7. **Purity of the exhaust N_2.** Time evolution of mass spectrometry signals of relevant species in the gas evolved from the anode (the working electrode) upon changing the cell voltage at a sweep rate of 0.33 mV/sec is shown. Due to experimental limitations, detection of NO_2 (amu 46) was not undertaken. Measurement was performed with humidified ammonia, pNH$_3$ = 0.4, pH$_2$O = 0.38, balance N_2, supplied to the working electrode and humidified hydrogen supplied to the counter electrode, exactly matching the conditions of Figure 2(a) of the main text. H_2O and residual NH_3 were removed from the gas stream by passing the gas through a condenser before delivery to the mass spectrometer (Thermostar Pfeiffer GSD 301 T2).

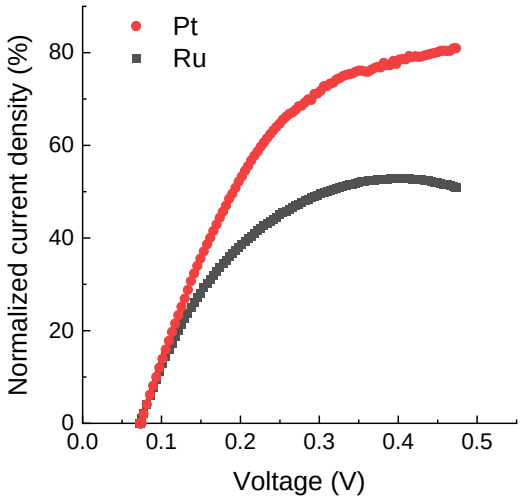

Figure S8. Polarization curves. Data collected (Biologic SP-300, scan rate of 10 mV/s) from electrochemical cells with a working electrode composed of M/CNT and CDP (CDP:CNT 1:9 by mass), where M is Pt or Ru as indicated. Humidified dilute hydrogen (pH$_2$ = 0.024 atm, pH$_2$O = 0.38 atm, balance Ar + N_2) is supplied to the working electrode, and humidified hydrogen is supplied to the counter electrode (pH$_2$O = 0.38 atm). For ease of comparison, raw current density is normalized against limiting current density (459 mA/cm^2 for Pt and 256 mA/cm^2 for Ru), where values differ between cells because of differences in active area. While the current density of the cell with the Pt-based electrode gradually approaches the limiting value, that of the cell with the Ru-based electrode peaks, and then declines at a voltage of ~ 0.38V. The behavior is tentatively attributed to H_2O poisoning of the Ru.

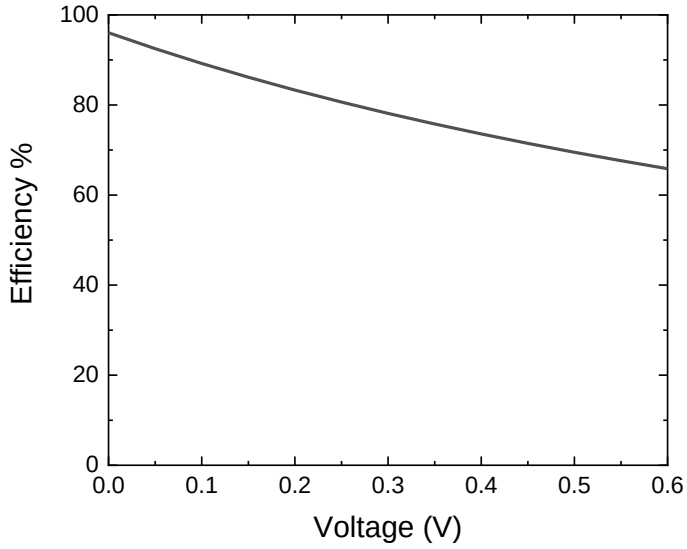

Figure S9. **Energy efficiency estimation**. The energy efficiency for the integrated thermal and electrochemical decomposition of ammonia to hydrogen using a solid acid cell is estimated assuming the output to be the work available from the generated hydrogen, and the input to be the work available from the consumed (not supplied) ammonia as well as the heat required to raise the temperature of the consumed ammonia to the operating temperature and to drive the reaction. For the energy content of the fuels, the lower heating values are used. No recovery of heat from the generated H_2 and N_2 is presumed. Similarly, the energy cost of heating steam and excess (non-reacted) ammonia is not considered. Thus, for the reaction

$$2NH_3 \xrightarrow[heat,electricity]{} 3H_2 + N_2$$

the efficiency is

$$\varepsilon = \frac{3\Delta H_{H_2,LHV}}{2\left(\Delta H_{NH_3,LHV} + \int_{298}^{523} C_p(NH_3)dT + \Delta_{rxn}H\right) + 6FV}$$

where F is Faraday's constant. Because overpotential losses increase monotonically with increasing voltage (V) and no penalty is assigned for the need to recycle un-utilized NH_3, the efficiency monotonically decreases in this calculation with increasing voltage (or equivalently, current density). The calculation does not account for the possibility of exploiting the exothermic electrical processes (cell resistance and overpotentials) to provide the thermal energy required for the endothermic dissociation reaction, which would increase the system efficiency.